

# Heat Transfer of slip boundary layer flow of non-Newtonian fluid over a flat plate with Viscous Dissipation

Shashidar Reddy Borra<sup>1</sup>

Department of Mathematics and Humanities,  
Mahatma Gandhi Institute of Technology,  
Gandipet, Hyderabad, Telangana State, INDIA.  
e-mail: bsreddy\_shashi@yahoo.com

Kishan Naikoti<sup>2</sup>

Department of Mathematics,  
Osmania University,  
Tarnaka, Hyderabad, Telangana State, INDIA.  
e-mail: kishan\_n@rediffmail.com

**Abstract**— This article numerically studies the effects of viscous dissipation and magnetic effects of an incompressible non-Newtonian power-law fluid over a flat plate convective thermal and slip boundary conditions. The governing boundary layer partial differential equations along with boundary conditions are first cast into a dimensionless form by a similarity transformation and the resulting ordinary differential equations are then solved numerically using implicit finite difference scheme. The solution takes Knudsen number  $Kn_x$ , heat transfer parameter, magnetic field parameter  $M$ , power-law fluid index  $n$ , Eckert number  $E_c$  and Prandtl number  $P_r$  effects into consideration. The influence of these parameters governing the flow on non-dimensional velocity and temperature fields are discussed graphically. The variation of the Knudsen number  $Kn_x$ , heat transfer parameter and Eckert number  $E_c$  on the skin friction, temperature at the wall and the rate of heat transfer is presented in tabular form.

**Keywords**- Magnetic field parameter, Knudsen number, Heat transfer parameter, Prandtl number, Viscous Dissipation and Non-Newtonian fluid)

## I. INTRODUCTION (HEADING 1)

The study of non-Newtonian fluid has been of much interest to scientist because some industrial materials are non-Newtonian such as in food, polymer, petrochemical, rubber, paint and biological industries, fluids with non-Newtonian behaviors are encountered. Of particular interest is power-law fluid for which the shear stress  $\tau$  is given by

$$\tau = \mu \left( \frac{\partial u}{\partial y} \right) = \mu_0 \left( \frac{\partial u}{\partial y} \right)^n, \text{ where } \mu = \mu_0 \left( \frac{\partial u}{\partial y} \right)^{n-1}$$

Where  $\mu_0$  is dynamic coefficient of viscosity,  $\frac{\partial u}{\partial y}$  is the

shear rate and  $n$  is the power-law index. When  $n < 1$  the fluid is pseudo-plastic, for  $n = 1$  the fluid is Newtonian and for  $n > 1$  the fluid is dilatant.

Some examples of a power-law fluid are commercial carboxymethyl cellulose in water, cement rocks in water, napalm in kerosene, lime in water, Illinois yellow clay in water. The studies of the flow of non-Newtonian fluids have over the past years attracted the keen interest of scientist. In

response to the pioneering papers of Sakiadis [1], several attempts for further developments in flow and heat transfer analysis have been reported in literature [2-5].

The study of non-Newtonian fluids with or without magnetic field has many applications in industries such as the flow of nuclear fuel slurries, liquid metal and alloys, plasma and mercury, lubrication with heavy oils and greases, coating of papers, polymer extrusion, continuous stretching of plastic films and artificial fibres and many others. The steady viscous incompressible flow of a non-Newtonian power-law fluid on a two-dimensional body in the presence of magnetic fields was studied by Sarpkaya [6]. The flow and heat transfer of a power-law fluid over a uniform moving surface with a constant parallel free stream in the presence of a magnetic field have been studied by Kumari and Nath [7]. Abo-Eldahab and Salem [8] have examined the Hall Effect on the MHD free convection flow of a non-Newtonian power-law fluid on a stretching surface. In recent years, the study of boundary layer flows of non-Newtonian fluids has increased considerably due to their relevance in scientific and technological applications such as oil recovery, material processing, soil, ceramics, lungs and kidney. In all these situations, one or more extensive quantities are transported through the solid and/or the fluid phases that together occupy a medium. Cheng has studied the natural convection heat and mass transfer of non-Newtonian power-law fluids in porous media [9].

The important experiment by Beavers and Joseph [2] established that when a fluid flows in a parallel plate porous channel, then a velocity slip at the porous wall is proportional to the wall velocity gradient. These observations have led to many publications in non-Newtonian heat and mass transfer, especially the pseudo plastic fluids [10, 11]. Kishan and Shashidar Reddy [12] studied the MHD effects on boundary layer flow of power-law fluids past a semi infinite flat plate with thermal dispersion.

Recently Ajadi et al [13] studied the flow and heat transfer of a power law fluid over a flat plate with convective thermal and slip boundary conditions. The purpose of this present work is study the viscous dissipation effects on the flow and heat transfer of a power law fluids in boundary

layer over a flat plate using the combination of slip boundary conditions and the convective thermal boundary condition.

II. MATHEMATICAL FORMULATION

Consider steady two-dimensional boundary layer flows of an incompressible non-Newtonian power-law fluid over a flat plate in a stream of cold fluid at temperature  $T_\infty$  moving over the top surface of the flat plate with a uniform velocity  $U_\infty$ . X-axis is taken along the direction of the flow and Y-axis normal to it. The schematic diagram of the boundary layer flows is as shown in figure 1.

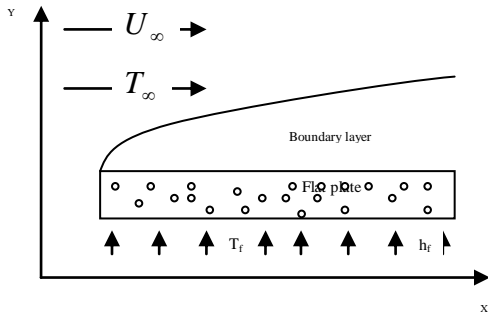


Figure 1: Sketch of the physical model

Also, a magnetic field of strength  $B$  is applied in the positive  $y$ -direction, which produces magnetic effect in the  $x$ -direction. Thus, the continuity, momentum and energy equations describing the flow can be written as

$$\frac{\partial u}{\partial x} + \frac{\partial v}{\partial y} = 0, \tag{1}$$

$$u \frac{\partial u}{\partial x} + v \frac{\partial u}{\partial y} = \nu \frac{\partial}{\partial y} \left( \frac{\partial u}{\partial y} \right)^n + g\beta(T - T_\infty) - \frac{\sigma B^2}{\rho} u, \tag{2}$$

$$\rho c_p \left( u \frac{\partial T}{\partial x} + v \frac{\partial T}{\partial y} \right) = k \frac{\partial^2 T}{\partial y^2} + Q(T - T_\infty) + \mu \left[ \frac{\partial u}{\partial y} \right]^{n+1} \tag{3}$$

The flow velocity boundary conditions associated with this problem can be expressed as

$$u(x, 0) = \frac{2 - F_M}{F_M} \lambda \frac{\partial u}{\partial y}, \tag{4}$$

$$v(x, 0) = 0 \text{ and } u(x, \infty) = U_\infty$$

Similarly, assuming that the flat plate is heated from below by a hot fluid whose temperature is maintained at  $T_f$ , with heat transfer coefficient  $h_f$ , then the boundary condition at the plate surface and beyond the boundary layer may be written as

$$-k \frac{\partial T}{\partial y}(x, 0) = h_f [T_f - T(x, 0)] \tag{5}$$

$$\text{and } T(x, \infty) = T_\infty$$

Where  $u$  and  $v$  are velocities along the  $x$ -axis (along the plate) and the  $y$ -axis (normal to the plate) components respectively,  $T$  is the temperature,  $\nu$  is the kinematic viscosity of the fluid and  $k$  is the coefficient of conductivity of the fluid,  $q_r$  is the radiative heat flux,  $\rho$  is the density and  $c_p$  is the specific heat capacity,  $Q$  is the heat source coefficient,  $B$  is the magnetic field strength,  $\mu$  is the magnetic permeability,  $\sigma$  is the electric conductivity,  $\beta$  is the coefficient of thermal expansion,  $g$  is the acceleration due to gravity,  $F_M$  is the momentum equation accounts for natural convection and the presence of magnetic field, while the energy equation accounts for the heat and radiative sources.

III. METHOD OF SOLUTION

We shall transform equation (03) and (04) into a set of coupled ordinary differential equation amenable to a numerical solution. For this purpose we introduce a similarity variable  $\eta$  and a dimensionless stream function  $f(\eta)$  defined as

$$\left. \begin{aligned} \eta &= y \left( \frac{U_\infty^{2-n}}{\nu x} \right)^{\frac{1}{n+1}} = \frac{y}{x} \text{Re}_x^{\frac{1}{n+1}}, & u &= U_\infty \frac{\partial f}{\partial \eta} = U_\infty f'(\eta) \\ v &= \frac{1}{n+1} x^{\frac{-n}{n+1}} \left( U_\infty^{2-n} \nu \right)^{\frac{1}{n+1}} (\eta f'(\eta) - f(\eta)), & \theta(\eta) &= \frac{T - T_\infty}{T_w - T_\infty} \end{aligned} \right\} \tag{6}$$

Using this in equations (03) & (04), we obtain the following coupled non-linear differential equations

$$n(f'')^{n-1} f''' + \frac{1}{n+1} f f'' + G_r \theta - M f' = 0 \tag{7}$$

$$\frac{1}{P_r} \theta'' + \frac{1}{n+1} f \theta' + \gamma \theta + E_c (f'')^{n+1} = 0 \tag{8}$$

$$\left. \begin{aligned} f(0) &= 0, f'(0) = \alpha \text{Kn}_x f''(0), & f'(\infty) &= 1, \\ \theta(\infty) &= 0, & \theta'(0) &= -\phi[1 - \theta(0)] \end{aligned} \right\} \tag{9}$$

Where

$$\text{Re}_x = \frac{x^n U_\infty^{2-n}}{\nu}, G_r = \frac{g\beta(T_\infty - T_w)x}{U_\infty^2}, M = \frac{\sigma B^2 x}{\rho U_\infty}$$

$$\gamma = \frac{Qx}{\rho c_p U_\infty}, \phi = \frac{h_f}{k} \sqrt{\frac{\gamma x}{U_\infty}}, P_r = \frac{\gamma \rho c_p}{kx} \left( \frac{\gamma x}{U_\infty^{2-n}} \right)^{\frac{2}{n+1}}$$

$$\text{Kn}_x = \frac{\lambda}{x} \text{ and } \alpha = \frac{F_M - 2}{F_M}$$

The dimensionless quantities  $G_r$  is the Grashoff number,  $P_r$  is the Prandtl number,  $M$  is the magnetic parameter,  $\text{Kn}_x$  is the Knudsen number,  $\alpha$  is the ratio of accommodation

factor,  $\phi$  is the heat transfer coefficient and  $\gamma$  is the heat source parameter.

IV. NUMERICAL PROCEDURE

The collective effects of various physical parameters will have great impact on heat transfer characteristics. The non-linearity of the basic equations and additional mathematical difficulties associated with the solution part has led us to use the numerical technique. In this section, an capable implicit finite difference scheme along with Quasi-linearization technique has been employed to analyze the flow model for the above coupled non-linear ordinary differential equations (7) and (8) along with the boundary conditions (79) for different values of the governing parameters. The transformed non-linear differential equation (7) is first linearized by Quasi-linearization technique discussed by Bellman and Kalaba [14]. Now by applying implicit finite difference scheme, these equations are transformed to system of linear equations. To carry out the computational procedure, first the momentum equation is solved which gives the values of  $f$  necessary for obtaining the solution of coupled energy and concentration equations under the boundary conditions (12) by Gauss Seidal iteration procedure. The numerical solutions of  $f$  are considered as  $(n+1)^{th}$  order iterative solutions and  $F$  are the  $n^{th}$  order iterative solutions. To prove convergence of finite difference scheme, the computation is carried out for slightly changed value of  $h$  by running same program. No significant change was observed in the value. After each cycle of iteration the convergence check is performed, and the process is terminated when  $|F - f| < 10^{-6}$ .

V. SKIN FRICTION

The shearing stress on the surface is defined by

$$\tau_w = \mu \left. \frac{\partial u}{\partial y} \right|_{y=0} \text{ -----(10)}$$

Thus the skin friction coefficient is defined by

$$C_f = \frac{2\tau_w}{\rho U_\infty} = 2 \text{Re}_x^{\frac{-1}{n+1}} [f''(0)]^n, \text{ -----(11)}$$

VI. HEAT TRANSFER

The local Nusselt number for heat transfer is defined by

$$N_u = \frac{v q_w}{k(T_\infty - T_w)} = -v x^{-1} \text{Re}_x^{\frac{1}{n+1}} \theta'(0), \text{ -----(12)}$$

Where the heat flux at the wall is given by

$$q_w = -k \left. \frac{\partial T}{\partial y} \right|_{y=0}$$

VII. RESULTS AND DISCUSSIONS

In order to carryout subsequent analysis of the effects of different flow parameters and to investigate the influence power-law indexes of non-Newtonian fluids over a flat plate with thermal boundary condition, numerical solutions are obtained for  $f'(\eta)$ ,  $\theta(\eta)$  and  $\theta'(\eta)$  for the different flow parameters Knudsen number  $Kn_x$ , Heat transfer coefficient  $\phi$ , magnetic field parameter  $M$ , power-law index  $n$ , Eckert number  $E_c$  and Prandtl number  $P_r$ . With the knowledge of  $f'(\eta)$ ,  $\theta(\eta)$  and  $\theta'(\eta)$  the skin friction coefficient  $f''(0)$ , temperature  $\theta(0)$  and the rate of heat transfer coefficient  $\theta'(0)$  are computed.

Numerical values are tabulated for  $f''(0)$ ,  $\theta(0)$ ,  $\theta'(0)$  for various values of Knudsen number  $Kn_x$ , Heat transfer coefficient  $\phi$  and Eckert number  $E_c$  for both pseudo plastic ( $n = 0.5$ ) and Newtonian fluid ( $n = 1.0$ ) in Tables 1-6. Table 1 and 4 shows that the skin friction coefficient  $f''(0)$  decreases with the increase in the Knudsen number  $Kn_x$  whereas, it has no effect with the change in heat transfer coefficient  $\phi$  and Eckert number  $E_c$  which is shown in tables 2,3, 5 and 6 for both pseudo-plastic ( $n = 0.5$ ) and Newtonian fluids ( $n = 1.0$ ). It is seen that the values of skin friction coefficient are higher for pseudo-plastic fluids ( $n = 0.5$ ) than the Newtonian fluids ( $n = 1.0$ ). From tables 1 and 4 show that temperature at the wall  $\theta(0)$  decrease with the increase in the Knudsen number  $Kn_x$  with and without radiation. The temperature at the wall  $\theta(0)$  increases with the increase in the heat transfer coefficient  $\phi$  and Eckert number  $E_c$  for both pseudo-plastic ( $n = 0.5$ ) and Newtonian fluids ( $n = 1.0$ ) which is shown in tables 2, 3, 5 and 6. The variation of  $-\theta'(0)$  with  $Kn_x$  and  $\phi$  are shown in tables 1,2, 4 and 5. It is evident from the tables that  $-\theta'(0)$  value increases with the effect of  $Kn_x$  and  $\phi$  for both pseudo-plastic ( $n = 0.5$ ) and Newtonian fluids ( $n = 1.0$ ). From the tables 3 and 6 it is seen that effect of Eckert number  $E_c$  is to decrease  $-\theta'(0)$  value for both pseudo-plastic ( $n = 0.5$ ) and Newtonian fluids ( $n = 1.0$ ). Figure 1 show that the dimensionless velocity profiles  $f'(\eta)$  increases with the increase of Knudsen number  $Kn_x$  for both pseudo-plastic ( $n = 0.5$ ) and Newtonian fluids ( $n = 1.0$ ). It is evident from these figures that the thermal boundary layer becomes thinner as  $Kn_x$  increases. Figure 2 show that with the effect of heat transfer coefficient  $\phi$  there is no variation in velocity profile  $f'(\eta)$  for both pseudo-plastic ( $n = 0.5$ ) and Newtonian fluids ( $n = 1.0$ ). The effect of magnetic field on the velocity profiles  $f'(\eta)$  is shown in the figure 3. It is evident from the figure that the magnetic

field effect is to decelerate the velocity profiles  $f'(\eta)$  for both the cases of pseudo-plastic ( $n = 0.5$ ) and Newtonian fluids ( $n = 1.0$ ).

The effect of Knudsen number  $Kn_x$  on the temperature profiles is shown in the figure 4, from which is observed that the temperature profiles decrease with the increase in Knudsen number  $Kn_x$  for both the cases of pseudo-plastic ( $n = 0.5$ ) and Newtonian fluids ( $n = 1.0$ ). The influence of heat transfer coefficient  $\phi$  is to increase the temperature profile  $\theta(\eta)$  in the both the cases of pseudo-plastic ( $n = 0.5$ ) and Newtonian fluids ( $n = 1.0$ ) which is shown in figure 5. It can be shown from the figure 6 that the influence of power-law index  $n$  is to reduce the velocity profile  $f'(\eta)$ . Whereas from the figure 7 it can be noticed that the temperature profiles  $\theta(\eta)$  increases with the increase in the power-law index  $n$ .

The influence of viscous dissipation on temperature profile  $\theta(\eta)$  is shown in figure 8. It is observed from the figures that temperature profiles increases with the increase of Eckert number  $E_c$  in both the cases of pseudo-plastic ( $n = 0.5$ ) and Newtonian fluids ( $n = 1.0$ ). It is also noticed that viscous dissipation effect is more in pseudo-plastic fluids ( $n = 0.5$ ) when compared with the Newtonian fluids ( $n = 1.0$ ). Figure 9 is drawn for temperature profiles  $\theta'(\eta)$  for pseudo-plastic ( $n = 0.5$ ) and Newtonian fluids ( $n = 1.0$ ). With the increase of Knudsen number  $Kn_x$   $\theta'(\eta)$  decreases near the boundary layer up to a certain extent and there after it will increase for both the cases of pseudo-plastic ( $n = 0.5$ ) and Newtonian fluids ( $n = 1.0$ ).

Figure 10 is drawn for temperature profile  $\theta'(\eta)$  for various values of heat transfer coefficient  $\phi$  in both the cases of pseudo-plastic ( $n = 0.5$ ) and Newtonian fluids ( $n = 1.0$ ). It can be seen that the effect of heat transfer coefficient  $\phi$  is to reduce the temperature profiles  $\theta'(\eta)$  in all the cases. It is observed that  $\theta'(\eta)$  is zero always in the absence of heat transfer coefficient  $\phi$ . The effect of viscous dissipation on temperature profiles  $\theta'(\eta)$  is shown in figure 11. The viscous dissipation effect is to increase the temperature profiles  $\theta'(\eta)$  near the plate whereas a reverse phenomenon could be seen far away from the plate for both the cases of pseudo-plastic ( $n = 0.5$ ) and Newtonian fluids ( $n = 1.0$ ).

The influence of prandtl number on the dimensionless temperature profile  $\theta'(\eta)$  for pseudo-plastic fluids ( $n = 0.5$ ) is shown in figure 12. It is seen from that temperature profiles  $\theta'(\eta)$  decreases near the thermal boundary layer and it increases after certain distance with increase in the prandtl number. It is notices that at far away from the plate  $\theta'(\eta)$  is zero.

## CONCLUSIONS

To summarized, the present investigation analyses the heat transfer of a power-law fluid flow over a flat plate with convective thermal and slip boundary condition considering the effects of viscous dissipation. From the above study, the following conclusions may be drawn:

1. The effect of Knudsen number is to accelerate the velocity and reduce the temperature.
2. Temperature rises with the heat transfer parameter and Eckert number.
3. The effect of power-law index is to reduce the velocity and increase the temperature.
4. The higher the Knudsen number, the lower is the skin friction.
5. Nusselt number increases with the increase in Knudsen number and heat transfer parameter.

## REFERENCES

- [1] B. C. Sakiadis, "Boundary layer behavior on continuous surfaces: Boundary layer equations for two dimensional and axisymmetric flow", A.I.Ch.E. J., vol. 7, pp. 26-28, 1961.
- [2] D. A. Nield, "The Beavers Joseph boundary condition and related matters: A historical and critical Note", Transp. Porous Med., vol. 78, pp. 537-540, 2009.
- [3] D. A. Nield, A. V. Kuznetsov, "Boundary layer analysis of forced convection with a plate and porous substrate", Acta Mechanica, vol. 166, pp. 141-148, 2003.
- [4] A. Aziz, "A Similarity solution for laminar thermal boundary layer over a flat plate with a convective surface boundary condition", Commun. Nonlinear Sci. Numer. Simulat., vol. 14, pp. 1064-1068, 2009.
- [5] R. B. Cortell, "Radiation effect in the Blasius flow", Applied Mathematics and Computation, vol. 198, pp. 333-338, 2008.
- [6] T. Sarpkaya, "Flow of non-Newtonian fluids in a magnetic field", A.I.Ch.E.J., vol. 7, 324-328, 1961.
- [7] M. Kumari and G. Nath, "MHD boundary layer flow of a non-Newtonian fluid over a continuously moving surface with parallel free stream", Acta Mech., vol. 146, pp. 139-150, 2001.
- [8] E. M. Abo-Eldahab and A. M. Salem, "Hall effect on MHD free convection flow of a non-Newtonian power-law fluid at a stretching surface", Int. Commun. Heat Mass Transfer, vol. 31, pp. 343-354, 2004.
- [9] C. Y. Cheng, "Natural convection heat and mass transfer of non-Newtonian power-law fluids with yield stress in porous media from a vertical plate with variable wall heat and mass fluxes", International Journal in Heat and Mass transfer, vol. 33, pp. 1156-1164, 2006.
- [10] M. Guedda and Z. Hammouch, "Similarity flow solutions of a non-Newtonian power-law fluid", Int. J. Nonlinear Sci., Vol 6(3), pp. 255-264, 2008.
- [11] B. I. Olajuwon, "Flow and natural convection heat transfer in a power-law fluid past a vertical plate with heat generation", Int. J. Nonlinear Sci., vol. 7(1), pp. 50-56, 2009.
- [12] N. Kishan and B. Shashidar Reddy, "Quasi linear approach to MHD effects on boundary layer flow of power-law fluids past semi infinite flat plate with thermal dispersion", International journal of non linear science, vol. 11(3), pp. 301-311, 2011.
- [13] S. O. Ajadi and A. Adegoke, A Aziz, "Slip Boundary layer flow of non-Newtonian fluid over a flat plate with convective thermal boundary condition", Int. J. Nonlinear Sci., vol. 8(3), pp. 300-306, 2009.
- [14] R. E. Bellman and R. E. Kalaba, Quasi-Linearization and Non-linear boundary value problems, New York: Elsevier, 1965.

**Table 1:**  $M = 0.1, \gamma = 0.1, \phi = 1, n = 0.5, G_r = 0, Ec = 0.0$

$Kn_x$	$f''(0)$	$Pr = 0.72$	
		$\theta(0)$	$-\theta'(0)$
0	0.163284	0.869726	0.130274
1	0.154233	0.842309	0.157691
2	0.142576	0.823169	0.176831
3	0.130896	0.809406	0.190594
4	0.120207	0.799132	0.200868
5	0.110753	0.791188	0.208812
6	0.102491	0.784859	0.215141
7	0.095278	0.779689	0.220311

**Table 4 :**  $M = 0.1, \gamma = 0.1, \phi = 1, n = 1.0, G_r = 0, Ec = 0.0$

$Kn_x$	$f''(0)$	$Pr = 0.72$	
		$\theta(0)$	$-\theta'(0)$
0	0.130829	0.922079	0.077921
1	0.122689	0.897537	0.102463
2	0.113236	0.880278	0.119721
3	0.103921	0.867827	0.132173
4	0.095364	0.858572	0.141428
5	0.087740	0.851490	0.148510
6	0.081031	0.845928	0.154072

**Table 2:**  $M = 0.1, \gamma = 0.1, Kn_x = 1, n = 0.5, G_r = 0, Ec = 0.0$

$\phi$	$f''(0)$	$Pr = 0.72$	
		$\theta(0)$	$-\theta'(0)$
0.1	0.154233	0.348174	0.065183
0.2	0.154233	0.516513	0.096697
0.4	0.154233	0.681184	0.127526
0.6	0.154233	0.762183	0.14269
0.8	0.154233	0.810363	0.15171
1.0	0.154233	0.842309	0.157691
1.5	0.154233	0.889040	0.166439
2.0	0.154233	0.914406	0.171188

**Table 5 :**  $M = 0.1, \gamma = 0.1, Kn_x = 1, n = 1.0, G_r = 0, Ec = 0.0$

$\phi$	$f''(0)$	$Pr = 0.72$	
		$\theta(0)$	$-\theta'(0)$
0.1	0.122689	0.466941	0.053306
0.2	0.122689	0.636619	0.072676
0.4	0.122689	0.777968	0.088813
0.6	0.122689	0.840148	0.095911
0.8	0.122689	0.875120	0.099904
1.0	0.122689	0.897537	0.102463
1.5	0.122689	0.929276	0.106086
2.0	0.122689	0.946002	0.107996

**Table 3:**  $M = 0.1, \gamma = 0.1, Kn_x = 1, \phi = 1, n = 0.5, G_r = 0$

$Ec$	$f''(0)$	$Pr = 0.72$	
		$\theta(0)$	$-\theta'(0)$
0.0	0.154233	0.842309	0.157691
0.5	0.154233	0.994118	0.005882
1.0	0.154233	1.145928	-0.14593
2.0	0.154233	1.449540	-0.44954
5.0	0.154233	2.360401	-1.3604
10	0.154233	3.878493	-2.87849
20	0.154233	6.914677	-5.91468

**Table 6 :**  $M = 0.1, \gamma = 0.1, Kn_x = 1, \phi = 1, n = 1.0, G_r = 0$

$Ec$	$f''(0)$	$Pr = 0.72$	
		$\theta(0)$	$-\theta'(0)$
0.0	0.122689	0.897537	0.102463
0.5	0.122689	0.955540	0.044460
1.0	0.122689	1.013543	-0.01354
2.0	0.122689	1.129548	-0.12955
5.0	0.122689	1.477564	-0.47756
10.0	0.122689	2.057592	-1.05759
20.0	0.122689	3.217648	-2.21765

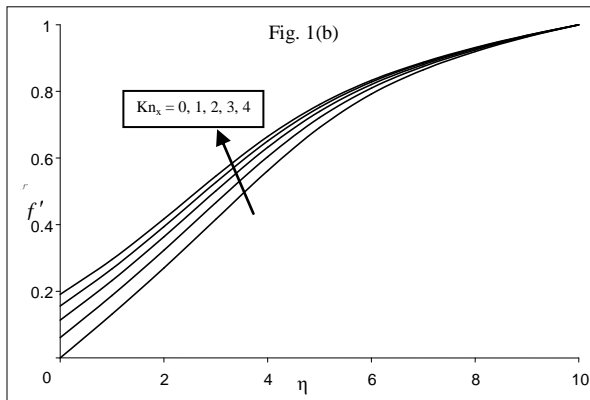
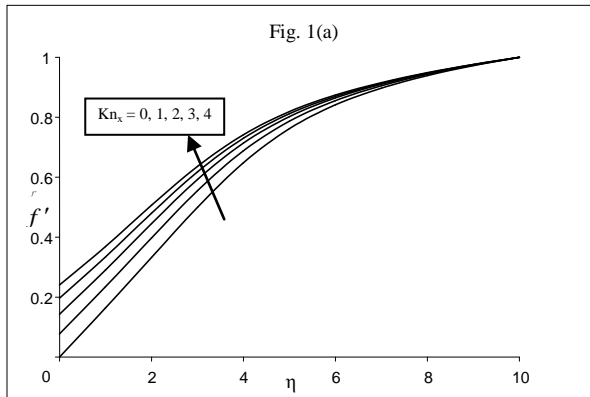


**Fig. 1** Velocity profiles for various values of Knudsen number  $Kn_x$  with  $\phi = 1$ ,  $P_r = 0.72$  and  $M = 0.1$ .  
 (a)  $n = 0.5$       (b)  $n = 1.0$

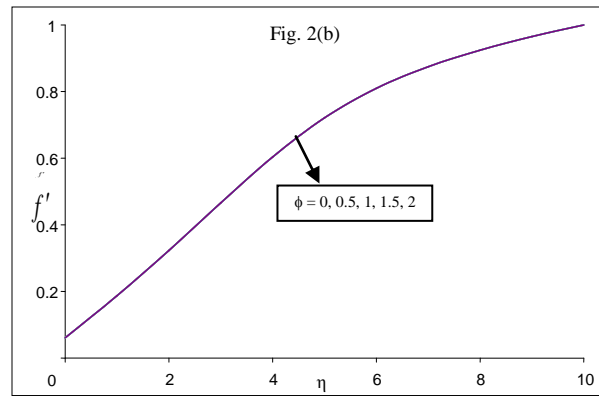
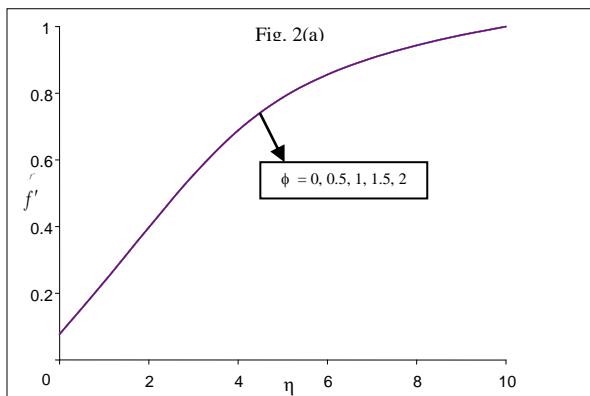


**Fig. 2** Velocity profiles for various values of heat transfer coefficient  $\phi$  with  $Kn_x = 1$ ,  $P_r = 0.72$  and  $M = 0.1$ .  
 (a)  $n = 0.5$       (b)  $n = 1.0$

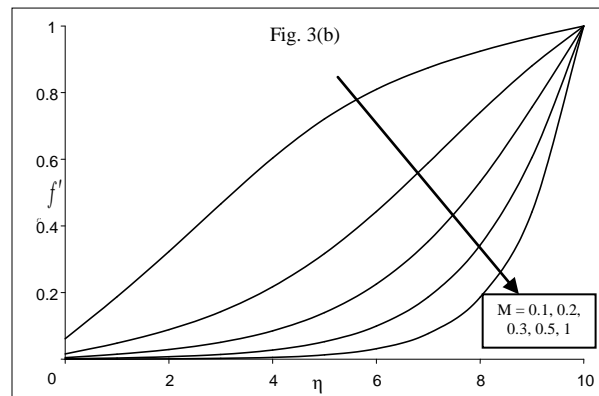
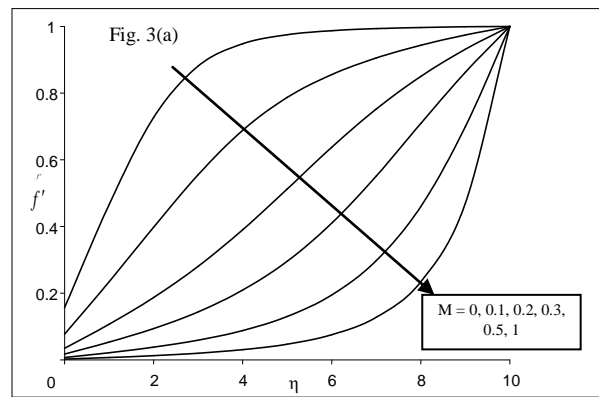


**Fig. 3** Velocity profiles for various values of Magnetic parameter  $M$  with  $Kn_x = 1$ ,  $\phi = 1$  and  $P_r = 0.72$ .  
 (a)  $n = 0.5$       (b)  $n = 1.0$

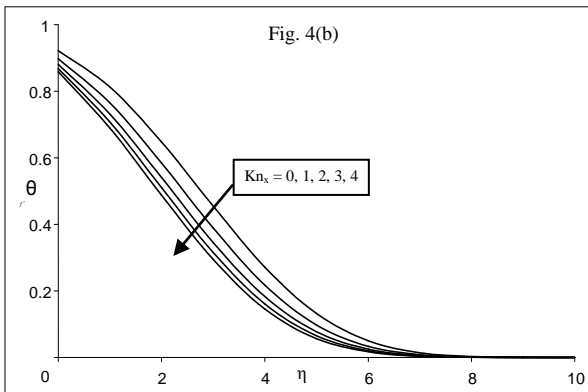
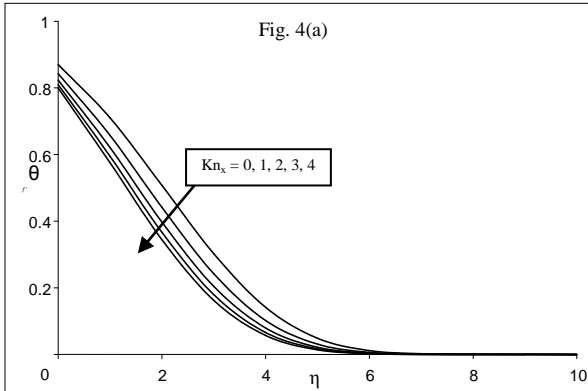


**Fig. 4** Temperature profiles for various values of Knudsen number  $Kn_x$  with  $\phi = 1$ ,  $P_r = 0.72$ ,  $E_c = 0$  and  $M = 0.1$   
**(a)**  $n = 0.5$       **(b)**  $n = 1.0$

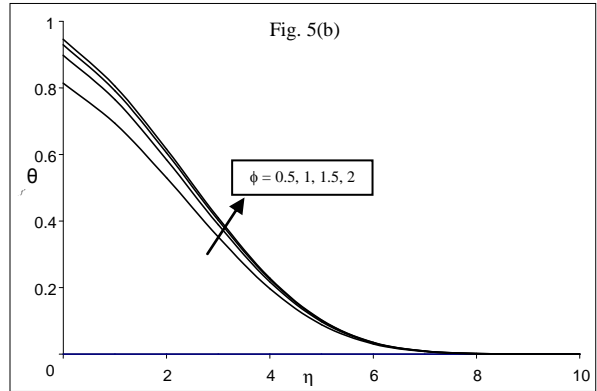
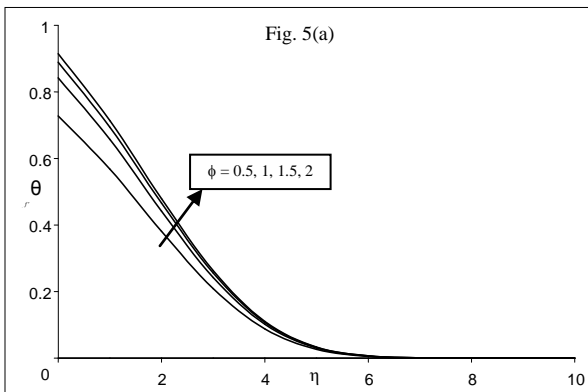


**Fig. 5** Temperature profiles for various values of heat transfer coefficient  $\phi$  with  $Kn_x = 1$ ,  $P_r = 0.72$ ,  $E_c = 0$  and  $M = 0.1$   
**(a)**  $n = 0.5$       **(b)**  $n = 1.0$

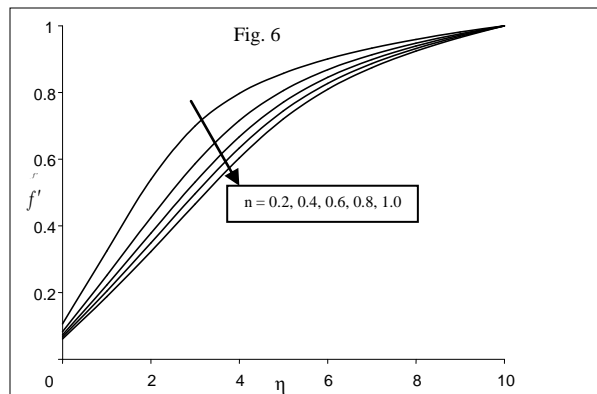


**Fig. 6** Velocity profiles for various values of power law index  $n$  with  $Kn_x = 1$ ,  $\phi = 1$ ,  $P_r = 0.72$  and  $M = 0.1$ .

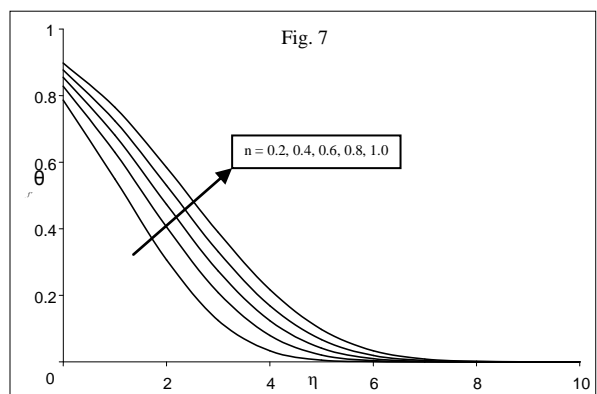


**Fig. 7** Temperature profiles for various values of power law index  $n$  with  $Kn_x = 1$ ,  $\phi = 1$ ,  $P_r = 0.72$ ,  $E_c = 0$  and  $M = 0.1$ .

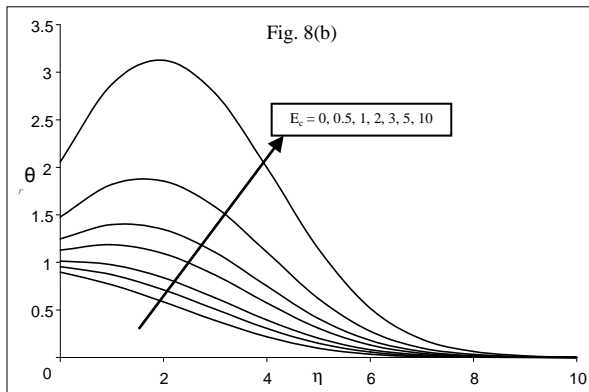
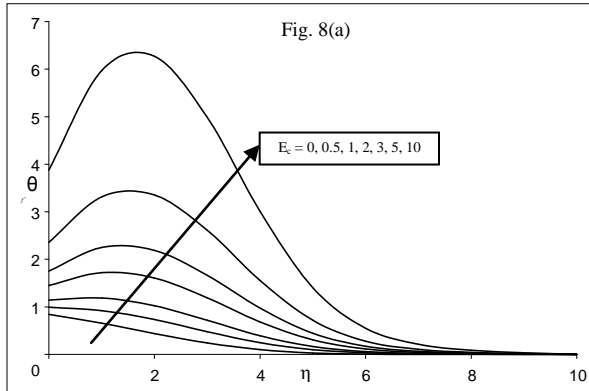


**Fig. 8** Temperature profiles for various values of Eckert number  $E_c$  with  $Kn_x = 1$ ,  $\phi = 1$ ,  $P_r = 0.72$  and  $M = 0.1$   
**(a)**  $n = 0.5$       **(b)**  $n = 1.0$

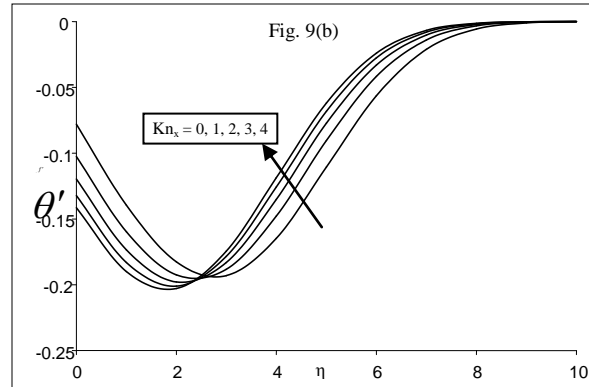


**Fig. 9** Temperature profiles  $\theta'(\eta)$  for various values of Knudsen number with  $\phi = 1$ ,  $P_r = 0.72$ ,  $M = 0.1$  and  $E_c = 0$   
**(a)**  $n = 0.5$       **(b)**  $n = 1.0$

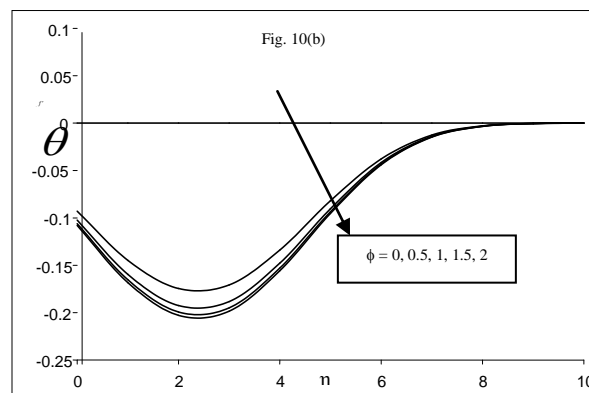
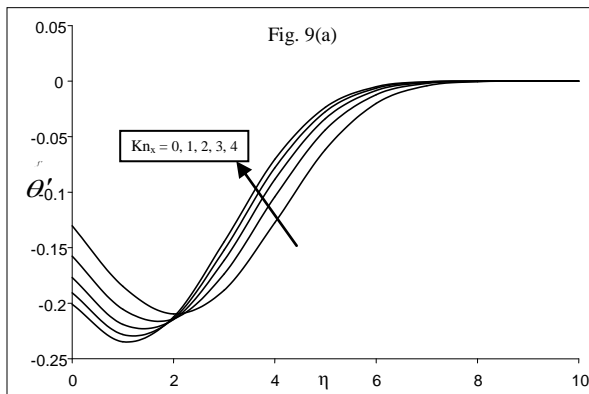
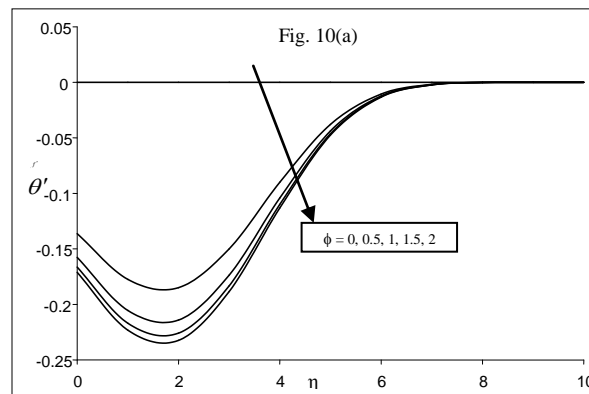


**Fig. 10** Temperature profiles  $\theta'(\eta)$  for various values of heat transfer coefficient  $\phi$  with  $Kn_x = 1$ ,  $P_r = 0.72$ ,  $M = 0.1$  and  $E_c = 0$   
**(a)**  $n = 0.5$       **(b)**  $n = 1.0$



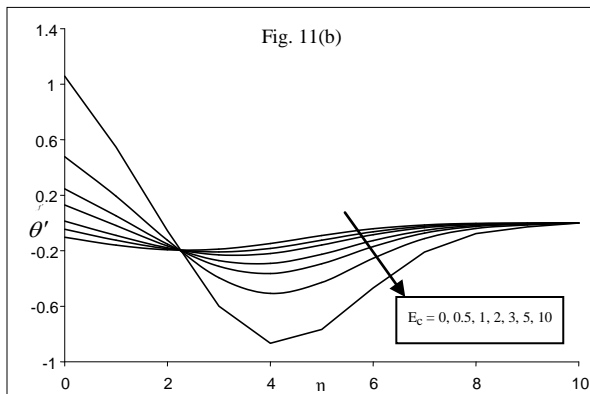
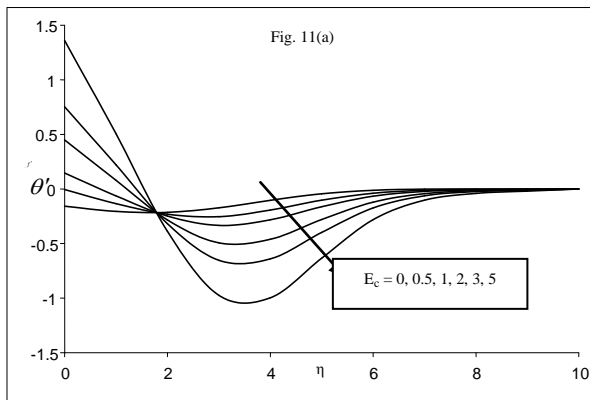


**Fig. 11** Temperature profiles  $\theta'(\eta)$  for various values Eckert number  $E_c$  with  $\phi=1$ ,  $Kn_x=1$ ,  $M=0.1$  and  $Pr=0.72$   
**(a)**  $n=0.5$       **(b)**  $n=1.0$

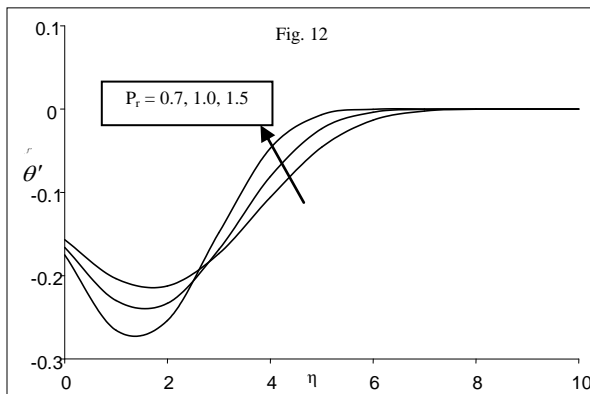


**Fig. 12** Temperature profiles  $\theta'(\eta)$  of pseudo plastic fluid for various values Prandtl number with  $\phi=1$ ,  $Kn_x=1$ ,  $M=0.1$  and  $E_c=0.0$